Journal of Materials Chemistry B

Zwitterionic Poly(Sulfobetaine Methacrylate) Hydrogels with Optimal Mechanical Properties for Improving Wound Healing In Vivo

Journal:	*Journal of Materials Chemistry B*
Manuscript ID	TB-ART-10-2018-002590.R3
Article Type:	Paper
Date Submitted by the Author:	17-Jan-2019
Complete List of Authors:	He, Huacheng; Wenzhou University, College of Chemistry and Materials Engineering Xiao, Zecong; Wenzhou Medical University, School of Pharmaceutical Sciences Zhou, Yajiao; Wenzhou Medical University, School of Pharmaceutical Sciences Chen, Anqi; Wenzhou Medical University, School of Pharmaceutical Sciences Xuan, Xuan; Wenzhou Medical University, School of Pharmaceutical Sciences Li, Yanyan; Wenzhou Medical University, School of Pharmaceutical Sciences Guo, Xin; Wenzhou Medical University, School of Pharmaceutical Sciences Zheng, Jie; University of Akron, Chemical and Biomolecular Engineering Xiao, Jian; Wenzhou Medical University, School of Pharmaceutical Sciences Wu, Jiang; Wenzhou Medical University, School of Pharmaceutical Sciences

Zwitterionic Poly(Sulfobetaine Methacrylate) Hydrogels with Optimal Mechanical Properties for Improving Wound Healing *In Vivo*

Huacheng He[1#], Zecong Xiao[2#], Yajiao Zhou[2], Anqi Chen[2], Xuan Xuan[2], Yanyan Li[2], Xin Guo[2], Jie Zheng[3]*, Jian Xiao[2]*, Jiang Wu[1]*

[1]College of Chemistry and Materials Engineering
Wenzhou University, Wenzhou, Zhejiang 325027, P.R. China

[2]School of Pharmaceutical Sciences
Wenzhou Medical University, Wenzhou, Zhejiang 325035, P.R. China

[3]Department of Chemical and Biomolecular Engineering
The University of Akron, Akron, OH 44325, USA

Corresponding Author: J.Z: zhengj@uakron.edu; J.X: xfxj2000@126.com; J.W. (woody870402@hotmail.com)

The authors contribute equally to this work

Abstract

Zwitterionic hydrogels, as highly hydrated and soft materials, have been considered as promising materials for wound dressing, due to their unique antifouling and mechanical properties. While the viscoelasticity and softness of zwitterionic hydrogels are hypothetically essential for creating adaptive cellular niches, the underlying mechanical-regulated wound healing mechanism still remains elusive. To test this hypothesis, we fabricated zwitterionic poly(sulfobetaine methacrylate) (polySBMA) hydrogels with different elastic modulus prepared at different crosslinker contents, and then applied the hydrogels to full-thickness cutaneous wounds in mice. *In vivo* wound healing studies compared the mechanical cue-induced effects of soft and stiff polySBMA hydrogels on wound closure rate, granulation tissue formation and collagen deposition. Collective results showed that the softer and more viscoelastic hydrogels facilitated cell proliferation, granulation formation, collagen aggregation, and chondrogenic ECM deposition. Such high wound healing efficiency by the softer hydrogels is likely attributed to stress dissipation by expanding cell proliferation the up-regulation of blood vessel formation, and the enhanced polarization of M2/M1 macrophages, both of which would provide more oxygen and nutrients for cell proliferation and migration, leading to enhanced wound repair. This work not only reveal a mechanical property-wound healing relationship of zwitterionic polySBMA hydrogels, but also provide a promising candidate and strategy for the next-generation of wound dressings.

Keywords: zwitterionic hydrogels, non-fouling, elastic modulus, protein adsorption, wound dressing

1. Introduction

Wound dressing is a key approach to address a grand challenge of wound healing for different traumatic, thermal, acute, and chronic wounds affecting millions of people globally[1]. Generally speaking, wound healing is a very sophisticated process that require different tissues and cells to cooperate and communicate in a way to realize cell proliferation and tissue remodeling (e.g. fibroblast migration, endothelial cell angiogenesis, and epithelial cell re-epithelization) after hemostasis and inflammation.[2] Despite of different wound types (e.g., traumatic, acute, chronic, exuding, and dry wounds), the design of nontoxic/nonallergenic wound dressings usually should satisfy several combinatory factors: protection of wounds from bacterial infection, high adsorption ability, improved cell proliferation, enhanced anti-inflammatory, desirable humidity environment, and/or ease of removal and replacement without pain.[3, 4]

Among different wound dressing materials, hydrogels are considered as the most promising wet-and-soft materials for wound dressing because their high water content, adequate mechanical/elastic, stimuli-responsive, and some self-recovery/self-healing properties[5-8], allowing them to well mimic wound soft tissues. Most of soft tissues (e.g. skin, blood vessel and nerves) not only possess high mechanical toughness and extensibility, but also exhibit the strain-induced viscoelastic behavior[9]. However, conventional hydrogels suffer from weak mechanical properties and poor mechanical responsive at different external stimuli[10], which greatly limits their uses as wound soft tissue substitutes. Extensive studies have reported that biomechanics of hydrogels and other soft materials (e.g. topographical and intrinsic structure, and mechanical toughness/strength/modulus/elasticity) is critical not only for serving as supporting substrates to retain tissue integrity and cell activity[11], but also for the transversion of biophysical cues to biochemical responses that regulate cell behaviors for tissue regeneration.[12] These cross-talk between biophysical and biochemical stimuli initiates cell proliferation, migration, differentiation, and remodeling during the wound healing process.[13, 14] Specifically, chemical (e.g. polymer components, crosslinkers) and mechanical (e.g. toughness, stiffness, modulus) properties of hydrogels (not limited to wound dressings) generally have influence on cell behaviors and wound repair effect.[15] For instance, hydrogels with optimal mechanical properties can better stimulate keratinocytes proliferation/migration, angiogenesis and neovascularization, and bFGF and TGF-β1 secretion, enhance blood vessel formation, re-epithelialization, extracellular matrix synthesis and remodeling, thus promoting

3

wound closure.[16, 17] Hydrogels with too low or too high stiffness will compromise the wound repair effect. These studies indicate that the presence of wound dressings allows cells to respond micromechanical stimuli at wound sites. On the other hand, cells can also rapidly produce extracellular matrix that will exert forces back to wound dressing materials.[18, 19] Apart from a chronic wound healing model, many previous studies have also shown that mechanical properties of hydrogels could be used and tuned to control and stimulate cell differentiation. [20, 21]

These hydrogel dressing examples have shown that biomechanics of biomaterials are pivotal for the fate, toxicity, and function of cells and tissues during wound healing process. However, there is a dearth of systematic research to better elucidate the poorly understood problem of how proteins and cells respond and adapt to hydrogel-based wound dressings. An in-depth address to this problem will provide mechanistic insights on the interactions between wound dressings and tissues at the hydrogel-wound interface, and thus promote the development of a new generation of wound dressings with long-term healing efficiency[22].

Significant research efforts have been made to develop poly(ethylene glycol) PEG-based polymers for wound healing, however less attention is paid to zwitterionic materials, some of which have demonstrated their super low-fouling property *in vitro* and anti-inflammatory property *in vivo*. Zwitterionic polymers are among the most popular antifouling materials, because zwitterionic polymers can be more hydrophilic than PEG to strong attract a layer of water molecules for resisting unwanted protein adsorption that will further lead to inflammation at wounds[23]. Herein, we prepared zwitterionic sulfated poly(sulfobetaine methacrylate) (polySBMA) hydrogels and applied them to full-thickness excisional acute wound regeneration in mice, with a particular attention to wound healing efficiency in response to mechanical softness/stiffness of polySBMA hydrogels with elastic modulus ranging from a softness of 10 kPa to a hardness of 60 kPa. Collective results showed that the softer polySBMA hydrogels could speed up wound healing efficiently through the intrinsic elastic impulse to improve neovascularization. Thus, zwitterionic hydrogels exhibit great potential as promising wound dressings.

2. Materials and Methods

2.1. Materials

[2-(Methacryloyloxy)ethyl]dimethyl-(3-sulfopropyl)ammonium hydroxide(SBMA, Mn=279.35) as monomer, Poly(ethylene glycol) dimethacrylate (PEGDMA, Mn =550) as

crosslinker, and Photoinitiator Irgacure 2959 (I2959), as initiator, were all purchased from Sigma-Aldrich. Hematoxylin-eosin (HE) or Masson's Trichrome Stain Kit (Sigma-Aldrich, St. Louis, MO). Phosphate buffer saline (PBS) was purchased from Sigma-Aldrich. Horseradish peroxidase (HRP)-conjugated goat anti-human lgG(H+L) was purchased from Beijing Biosysthesis Biotechnology Co. Human umbilical vein endothelial cell (HUVEC) was purchased from the Cell Storage Center of Wuhan University (Wuhan, China). Other cell culture reagents were purchased from Invitrogen (Carlsbad, CA). Deionized water was used as received.

2.2. Preparation of polySBMA hydrogels with different elastic modulus

Different polySBMA hydrogel were prepared using the previous method[24]. Here the elastic modulus of polySBMA hydrogels was achieved by the chemical cross linker percentage. The monomer SBMA were firstly issolved in de-ionized DI water. The corss linker (PEGDMA) were varied from 0.1%, 0.5%, 1% to 5% (versus monomer w/w) and the initiator I2959 (final 1% versus monomer w/w) were added and complete dissolved to the above solutions at room temperature. The final concentration of the monomer is 4 M. Then the mix solution was transferred into a pair of glass plates separated by poly(tetrafluoroethylene) (PTFE) (with the thickness of 3 mm or 1 mm). Next, the photo-polymerization reaction was carried out under room temperature with 362 nm UV light SB-100P (Spectroline) for 30 mins. After the polymerization, the hydrogels were removed from the plates by immersing in a large volume of DI water (1 L), which was changed and kept in water every 3 h for 5 days to ensure that non-reacted initiators or monomers were totally removed from the hydrogel.

2.3. Determination of Equilibrium water content (EWC) of the hydrogels

The hydrated hydrogels were used to quantify its EWC by weighting their mass difference between the hydrated state and fully dried state. The weight of the hydrogels in swollen state recorded as Ws, the lyophilized dried hydrogel recorded as Wd. The EWC is determined by the weight change of hydrogel in swelling state and dry states using the following Eq. (1):

$$EWC\ (\%) = \frac{(Ws - Wd)}{Ws} \times 100\% \qquad (1)$$

The swelling kinetics of polySBMA hydrogels were tested using gravimetric method. Same size of prepared swollen hydrogels was firstly freed-dried Wd. Secondly immersed in the deionized water. At each time interval, the samples were wiped with filter paper to remove

the appearance water. The weight of the hydrogels was measured Wt. The degree of swelling ratio was calculated using the following Eq. (2):

$$\text{Swelling ratio (\%)} = \frac{Wt - Wd}{Wd} \times 100\% \quad (2)$$

The losing rate of the hydrogel varied by days was achieved by weighting hydrogels everyday recorded as We and the initial swollen hydrogel recorded as Wi. Then the water retaining content is obtained using following Eq. (3):

$$\text{Water retaining content (\%)} = \frac{Wi - We}{Wi} \times 100\% \quad (3)$$

2.4. Morphology of polySBMA hydrogels

The morphology of the hydrogels was examined by scanning electron microscopy (SEM). Swollen polySBMA hydrogel samples were firstly frozen in liquid nitrogen then lyophilized overnight for at least 24 h. Before SEM, the cross sectional part of dried hydrogel was coated with gold by ion sputtering. SEM analysis proceeded with an acceleration voltage of 10 keV and a probe current of 25 mA (Hitachi S-3000 SEM).

2.5. Compressive mechanical tests of hydrogels

Swollen hydrogels immersing in water for more than 5 days with cylindrical shape (8 mm in diameter and 3 mm in thickness) were placed on the compression plate. Five disks of each hydrogel were compressed to failure at a compressive strain rate at 1 mm/min using Instron 3343 (Instron Co, U.S.A) with a 10 N load cell at the room temperature. The modulus was calculated from the linear portion of the stress-strain curve.

2.6. Protein adsorption measurement

Nonspecific protein adsorption to hydrogels were determined by quantifying HRP-conjugated anti-IgG adsorption using Tissue culture polystyrene (TCPs) as control. The samples were firstly incubated with 1 μg/ml anti-IgG for 1.5 h followed by six times rinsing with PBS. The TCPs and the hydrogels were then removed to 24-well plates separately. Secondly, 1 ml o-phenylenediamine (OPD 1 μg/ml) in 0.1M citrate phosphate buffer (pH 5.0), containing 0.03% hydrogen peroxide was added. Next, this enzyme-substrate activity reaction was stopped by adding an equal volume of H_2SO_4 (2M) after 15 min. At last, the relative protein adsorption percentage compared to TCPs is measured by tangerine color at 492 nm.

2.7. In vitro HUVEC cell surface attachment assay

TCPs and polySBMA hydrogels were placed individually in the 24-well plates. Being irradiated under 30mins UV light, 10^5 cells/mL HUVEC cells were seeded onto the samples in RPMI 1640 medium. After the cells growing for 24 h at 37°C, 5% CO_2 and 100% humidity, the samples were photographed at 4 x Nikon Eclipse TE2000U microscope.

2.8. *In vivo* wound healing model and analysis

The animal models were followed by the same procedure as our previous paper[25]. 6 to 7 weeks male C57BL/6 mice weight 25 g were purchased from the Animal Center of Chinese Academy of Sciences, Shanghai, China. The experiment animals were carried out with the National Institutes of Health Guide Concerning the Care and Use of Laboratory Animals. All animal experiments were performed in accordance with the guidelines approved by the Animal Experimentation Ethics Committee of Wenzhou Medical University, Wenzhou, China. Mice were maintained for at least 7d before the experiment on a standard diet and water was provided freely available. Temperature (23 ℃ -25 ℃), humidity (35−60%), and photoperiod (12 h light/dark cycle) were kept constant. Firstly, the mouse were anaesthetized by an intraperitoneal injection of 4% chloral hydrate (0.1 ml/10g) and the dorsal area was shaved. 0.5-mm-thick silicone donut-shaped splints (the external diameter of 16 mm, the internal diameter of 8 mm) were fixed on either side of the dorsal midline using 6-0 Prolene suture. Two full-thickness cutaneous wounds were made using a 6 mm round skin biopsy punch (Acuderm® inc., Ft Lauderdale, FL, USA) on each side of the dorsal midline. Secondly, the wound site were measured using digital camera take photos to determine the original wound area. The wound was then treated with our sample hydrogels. Each sample used 7 animals with 14 wounds per group. All hydrogel dressings were cut into 7 mm diameter dish with punch immediately before applying to the wound. The hydrogels dressing was last covered with Tegaderm™ transparent dressing (3M Health Care, Germany) to prevent from infection and wrapped in a thin layer of self-adhesive bandages to deter chewing of the splints. At days 0, 7, 10, 14, and 17 post-treatment, the wound closure rate was determined by measuring the wound area by Image-Pro plus to trace the wound margin. (wound closure rate % = (wound area$_{day0}$ - wound area$_{day\#}$)/wound area$_{day0}$×100%). At day 7 or 20 post-surgery C57BL/6 mice were anesthetized with 4% chloral hydrate and sacrificed by cervical dislocation. The wound site was excised, and the tissue was processed for histological evaluation.

2.9. Histological analysis

For histological preparation the skin was fixed in 4% paraformaldehyde in 0.01M phosphate buffered saline (PBS, pH=7.4) overnight and dehydrated in graded ethanol series then embedded in paraffin. The tissue was sectioned into 5-μm thickness slices for Hematoxylin and Eosin (H&E) (Beyotime Institute of Biotechnology, China) staining and for collagen formation by Masson's trichrome staining (Beyotime), using standard reported procedures[26]. Sections were analyzed and images were captured using a Nikon ECLPSE 80i (Nikon, Japan).

2.10. Immunofluorescent staining

The CD-31 (ab28364, Abcam), Ki67(ab15580, Abcam), CD 163 (ab182422, Abcam) and CD 68(ab955, Abcam) were conducted by respective antibody the same with our previous paper.[23] The Skin tissue sections, prepared by a microtome to 5-μm thickness, were deparaffinized and rehydrated, and then immersed in 3% H_2O_2 and 80% carbinol for 15 min at room temperature to blocked the endogenous peroxidase activity. The tissue sections were heated to antigen recovery in 10 mM sodium citrate buffer (pH 6.0) and after washing the samples were blocked using 5% bovine serum albumin (BSA) (Beyotime) for 30 min at room temperature. Skin sections (on 7 day post wound) were stained with rabbit polyclonal anti-CD31 (1:200), anti-Ki67 (1:200), rabbit polyclonal anti-CD 163 (1:200) and mouse monoclonal anti-CD 68 (1:100) diluted in phosphate-buffered saline (PBS) contained 1% bovine serum albumin (BSA) overnight at 4°C. Fluorescence secondary antibodies IgG Alexa Fluor® 488 and goat anti-mouse IgG Alexa Fluor® 647 (ab150083, 1:1500, Abcam) were diluted with phosphate-buffered saline (PBS) respectively then incubated at 37°C for 60 min. Followed by DAPI stained nuclear 5 min and coverslipping with Anti-fluorescent quencher. The fluorescent images were taken by Nikon confocal laser microscope (Nikon, A1 PLUS, Tokyo, Japan).

2.11. Statistical Analysis

All the data were expressed as the means ± standard deviations (SD). The statistical data were compared using unpaired-student's t-test. Significant difference was considered if the two-tailed P-values were <0.05. For all test, *P<0.05, **P<0.01 and ***P<0.001.

3. Results and Discussion

3.1. Physicochemical properties of polySBMA hydrogels

To fabricate the hydrogels with controllable mechanical properties, here we used different crosslinking percentage (0.1%, 0.5%, 1%, and 5%) to tune polySBMA hydrogels from soft to stiff. **Figure 1A** represents the typical compressive strain-stress curves of polySBMA hydrogels. As crosslinkers increased from 0.1% to 5%, polySBMA hydrogels significantly and monotonically increased their compressive stress from 0.015 Mpa to 0.35 Mpa (**Figure 1A**) and elastic modulus from 6.7 kpa to 50.4 kpa (**Figure 1B**) at a compressive strain of 80% without broken. For the convenience of system notation, based on compressive mechanical properties of polySBMA hydrogels, polySBMA hydrogels with low elastic modulus of <12 kPa prepared at 0.1% and 0.5% crosslinkers are defined as soft-1 and soft-2 hydrogels, while the remaining two hydrogels with high elastic modulus of >48 kPa prepared at 1% and 5% are defined as stiff-1 and stiff-2 ones. **Figure 1C** also showed that on one hand, four polySBMA hydrogels were highly hydrated with consistent high EWC of > 80%, demonstrating the hydrophilic nature of polySBMA hydrogels. On the other hand, increase of crosslinker contents also slightly reduced EWC by 10% simply because of the more compact and tightly interpenetrating network. In parallel, **Figure 1D** shows the swelling kinetics of four hydrogels in PBS solution. It can be seen that all hydrogels swell rapidly to achieve equilibrium swelling within ~4 h. Consistently, increase of crosslinkers reduced hydrogel swelling, accordingly the swell ratios were 1392.2% for soft-1 (0.1%), 965.0% for soft-2 (0.5%), 542.8% for stiff-1 (1%), and 469.0% for stiff-1 (5%), respectively. This phenomenon became even more pronounced for soft-1 hydrogels, which swollen almost 3-times higher than stiff hydrogels. Thus, the introduction of crosslinkers enables to greatly suppress the expansion of gel networks. As expected, the swollen transparent hydrogels become mechanically weak, due to the breaking of hydrogen bonds and lower polymer volume fraction.
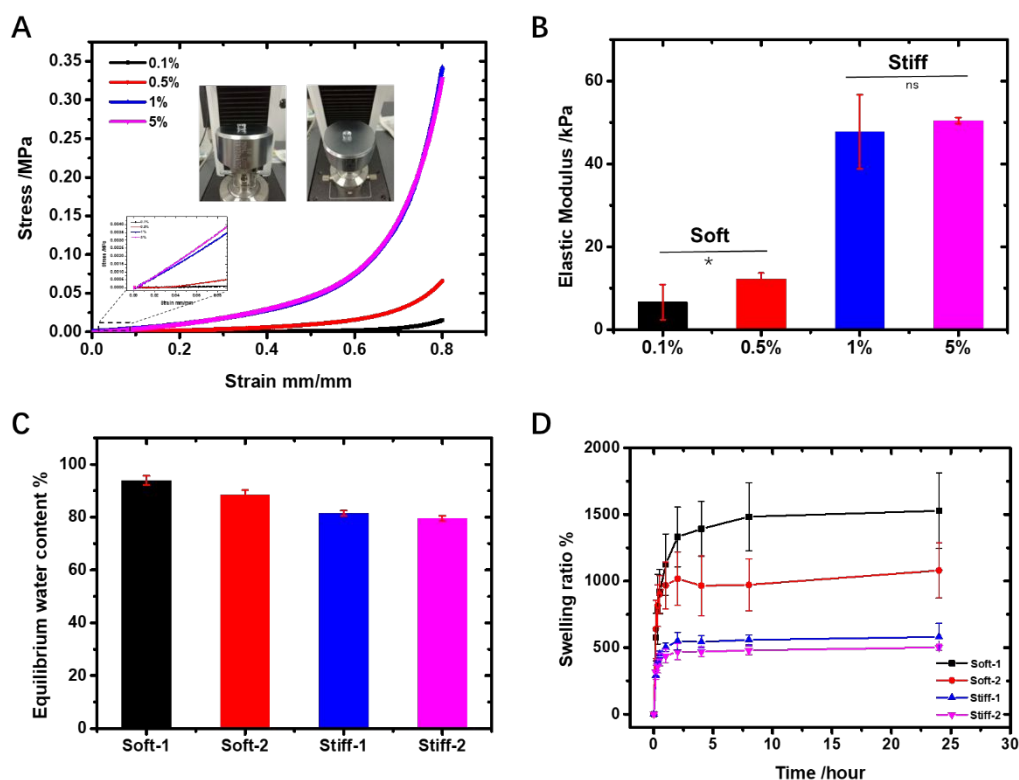
Figure 1. Compressive properties of zwitterionic polySBMA hydrogels prepared by different cross-linking density from 0.1% to 5%. (A) Compressive stress-strain curves, (B) Elastic modulus, (C) Equilibrium water content (EWC), and (D) Swelling kinetics of as-prepared polySBMA hydrogels.

Figure 2A showed the optical property of the four polySBMA hydrogels at the as-prepared state. Except for the stiff-2 hydrogel (5% of crosslinkers) showing semitransparent optical property, the other three hydrogels exhibited optical transparency. SEM images in **Figure 2B** showed the internal morphology of four polySBMA hydrogels. It can be seen clearly that each individual hydrogel possessed relatively uniform pore structure, but pore size distribution decreased from 20 µm to 5 µm as crosslinkers. The highly porous structures in all hydrogels resemble natural macromolecular cellar matrix systems, suitable for cells proliferation and migration, as well as oxygen permeation especially for chronic wound as wound dressing to improve neovascularization. **Figure 2C** showed that due to the strong ionic solvation of zwitterionic polymers, all polySBMA hydrogels enable to retain high water content of ~70% at room temperature for 7 days. Such high water retention property of Soft-1, Soft-2, Stiff-1 and Stiff-2 hydrogels makes advantages for keeping the wound site moist.
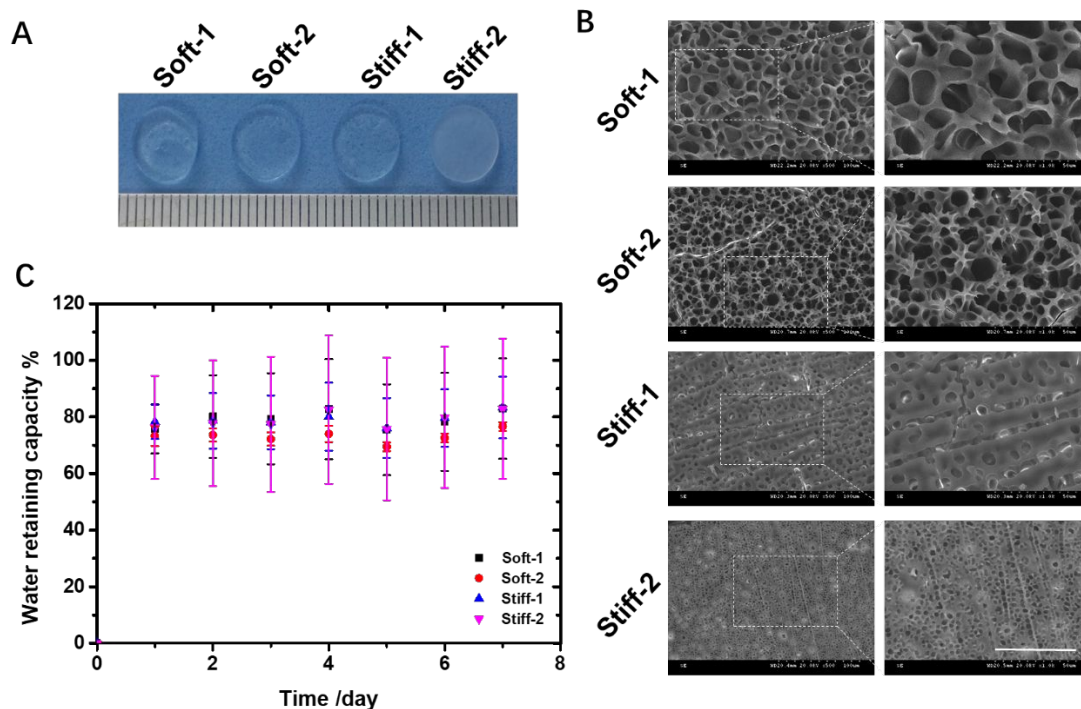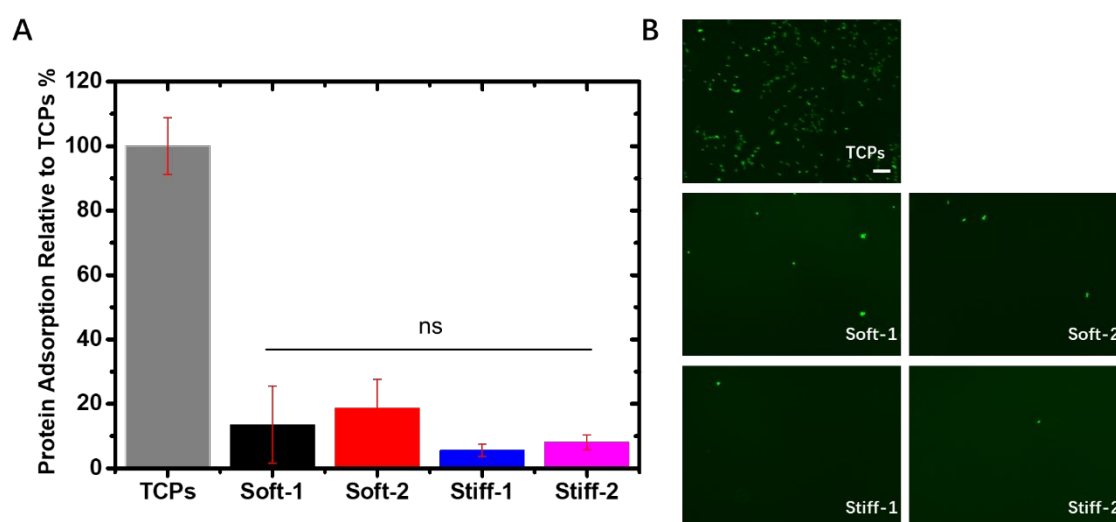
Figure 2. Physical properties of zwitterionic polySBMA hydrogels prepared at different cross-linking densities from 0.1% to 5% (namely as soft-1, soft-2, stiff-1, and stiff-2 hydrogels). (A) Visual inspection of appearance, (B) SEM images (scale bar=50 μm), and (C) water retaining capacity of the four polySBMA hydrogels.

3.2. *In vitro* antifouling properties of polySBMA hydrogels

Antifouling properties of polySBMA polymers are critical for wound healing[23]. Our previous work has demonstrated that polySBMA polymer brushes could achieve ultralow fouling level of protein adsorption (<0.3 ng/cm^{2}) and also excellent hydrophilicity, salt resistance, and biocompatibility[27-29]. Different from previous work focusing on antifouling property of polySBMA brushes, here we examined the protein adsorption on polySBMA hydrogels using enzyme-linked immunosorbent assay (ELISA), where tissue culture polystyrene (TCPs) was used as control to set a complete monolayer protein adsorption (100%). As shown in **Figure 3A**, as compared to TCPs, all polySBMA hydrogels significantly reduce adsorbed protein amounts to 5%-20%. Stiffer polySBMA hydrogels exhibited the slightly better protein resistance than softer hydrogels, probably because higher elastic modulus and the more compact porous structures prevent protein adsorption on and adaption to hydrogel surface[24]. Further data analysis results showed that under the consideration of error bar, no significant difference (ns) between soft (0.1% and 0.5%) and stiff (1% and 5%) hydrogels. To

11

further test the ability of polySBMA hydrogel to resist cell attachment, a cell assay was carried out to probe the additional antifouling property of the hydrogels. GFP-expressed HUVEC cells were used to co-culture with polySBMA hydrogels at 37° C for 24 h. After culturing, hydrogels were gently washed with PBS to remove any unbound or weakly bound cells. Finally, the images of four hydrogels were taken under a fluorescent microscope with the same excitation light and exposure time. As shown in **Figure 3B**, in sharp contrast to TCPs whose surface was covered by an almost full layer of cells, all polySBMA hydrogels exhibited neglectable cell attachment. Even though the polySBMA hydrogels had been soaked in serum-containing medium for two weeks, polySBMA hydrogels, regardless of their mechanical softness or stiffness, were able to kept their non-fouling property and did not allow cell adhesion on their surfaces, demonstrating their intrinsic nature of antifouling property.


Figure 3. Antifouling properties of zwitterionic polySBMA hydrogels prepared at different cross-linking density from 0.1% to 5%. (A) IgG protein adsorption and (B) Cell adhesion (scale bar=500 μm) on all polySBMA hydrogels relative to TCPs.

3.3. *In vivo* wound regeneration properties of polySBMA hydrogels

After polySBMA hydrogels have demonstrated their excellent antifouling properties to resist both protein adsorption and cell adhesion *in vitro*, here we applied polySBMA hydrogels to full-thickness cutaneous wounds in C57BL/6 mice, and then examined their wound efficiency as the effect of elastic modulus. At a first glance, both visual images of wound bed closure (**Figure 4A**) and the corresponding mimetic trace of wound bed closure (**Figure 4B**) were used to assess the in vivo wound-healing efficacy of the polySBMA hydrogels at different

time points during 20-days treatment. Compared to a control group treated with PBS, all polySBMA hydrogels showed the enhanced wound regeneration behavior and no obvious sign of inflammation or infection near the wound area. It appears that the growth of new epidermis extended to the center of all hydrogel treated wounds, resulting in a reduction in wounded area. Among four polySBMA hydrogel treated groups, the wounds treated by soft-1 and soft-2 hydrogels regenerated faster than stiff-1 and stiff-2 hydrogels. Specifically, after 20-days treatment, soft-1 and soft-2 polySBMA hydrogels enable to completely heal the wounds with almost scarless, while siff-1 and stiff-2 treated wounds still remained obvious residual wound area. Quantitatively, **Figure 4C** analyzed the restoration area ratio of wound bed. Consistent with visual inspection, soft-1 and soft-2 hydrogels showed significantly higher wound closure rate than stiff-1 and stiff-2 hydrogels at every check point of days. The final wound closure rates of soft hydrogels were 98.1% and 93.2%, as compared to those of stiff-1 (87.5%), stiff-2 (89.5%), and control (85.0%) hydrogels. The ~10% enhancement in wound regeneration of soft polySBMA hydrogels could be attributed to soft mechanical properties, high water content, and nanomorphological structures, all of which are more compatible with soft skin, thus providing a "suturing" effect at the wound site to enhance wound contraction and closure during the early stage of the wound-healing process. In **Figure 4C**, on day 20, there exists significant differences between soft-2 and stiff-1 gels and between soft-2 and stiff-2 gels, in which both p values were lower than 0.01 ("*" indicates $p < 0.05$). However, the results on day 17 did not show obvious improvement between soft-2 and stiff-1/stiff-2 gels. In general, both soft hydrogels showed significant enhancement of wound regeneration than both stiff hydrogels on day 17 and day 20. This result further confirms the wound healing efficiency is sensitive to the mechanical property of the hydrogels.
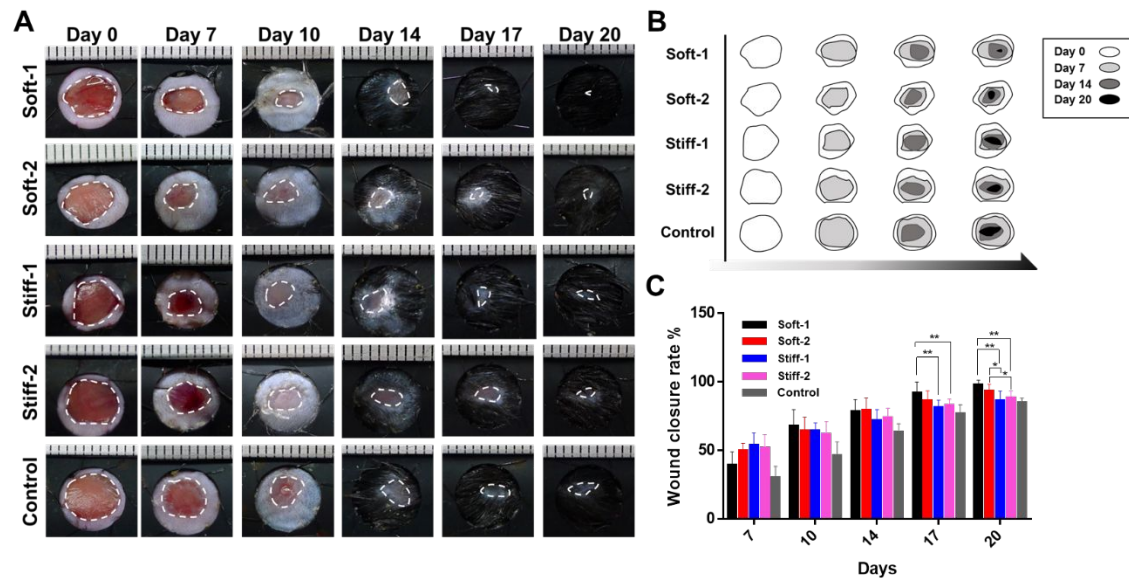
Figure 4. In vitro wound healing efficacy of zwitterionic polySBMA hydrogels prepared at different cross-linking densities. (A) photographs of excised wounds, (B) schematic of wound closure trace, and (c) quantitative evaluation of wound closure rate for all hydrogel- and saline (control)-treated wounds on day 0, 7, 10, 14, 17 and 20 in each group. Error bars indicate SD. Significant differences between sample means are indicated: ** P <0.01, * P <0.05 where n>6.

Considering that a typical wound healing process comprises granulation tissue formation, re-epithelialization, and collagen deposition, here we used the H&E staining of wound treated with polySBMA hydrogels on day 7 and day 20 to evaluate the granulation and epidermal formation. As shown in **Figure 5A**, H&E stained sections of the wounded skins treated with polySBMA hydrogels exhibited a markedly higher epidermis and granulation construction than that of control group. Specifically, on day 7, hydrogel-treated groups developed a full length of epidermal layer, while the control group induced the less epithelialization. On day 20, hydrogel-treated groups were able to connect tightly regenerated dermis and fill with appendants under a fully healed epithelialization layer, while the control group still had larger unhealed wound areas with a thin granulation construction. Similar to our earlier *in vivo* wound closure results, while the H&E staining for all groups showed no pathological changes, the softer hydrogels had the smaller wound closure area and the thicker granulation formation than the stiffer hydrogels. Furthermore, H&E staining was performed on the wound cross sections to identify and quantify at the center of the wound. (**Figure 5B**). The results show that the mean length of granulation gap at day 7/day 20 for wounds treated with wounds treated with soft-1, soft-2, stiff-1, stiff-2, and PBS was 3.0/1.2, 3.4/1.8, 3.8/2.5, 4.0/2.0

and 4.5/3.2 μm, respectively (**Figure 5C**). The mean granulation tissue thickness was with average 1.6/1.6, 1.5/1.3, 1.4/1.2, 1.3/1.2, and 1.0/0.7 μm for wounds treated with soft-1, soft-2, stiff-1, stiff-2, and PBS was at day 7/day 20, respectively (**Figure 5D**). Altogether, these results suggest that the softer polySBMA hydrogels significantly accelerate skin wound healing via improved granulation tissue formation and epithelial tissue regeneration, relative to the stiffer hydrogels.
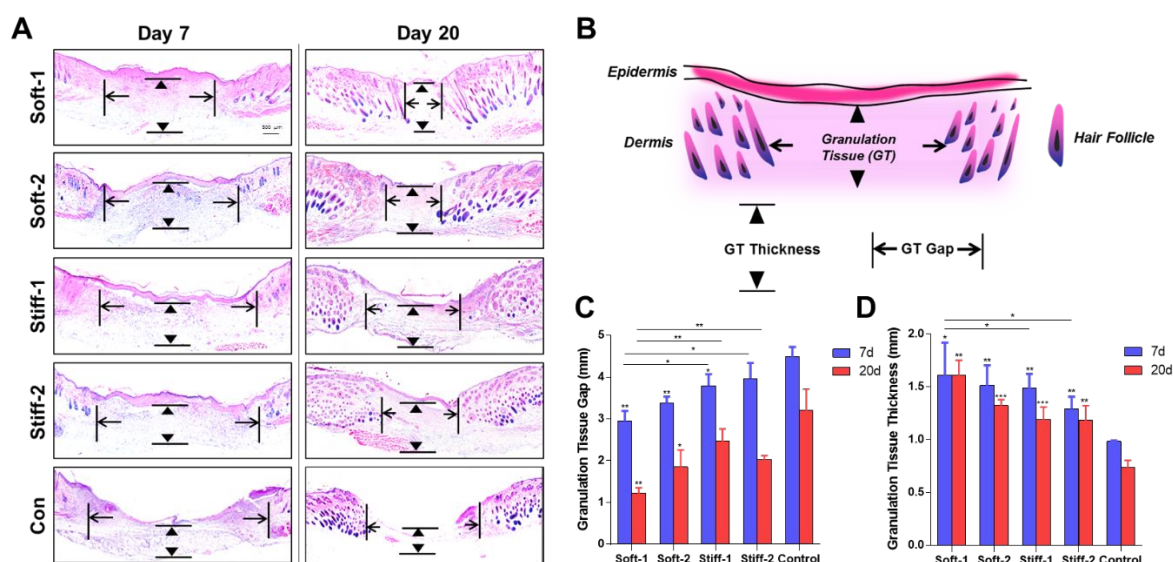
Figure 5. H&E staining of wound sections obtaining from different zwitterionic polySBMA hydrogels and control groups day 7 and day 20 post-operation. (A) H&E stained images for skin wounds treated with polySBMA hydrogels and PBS on day 7 and day 20. (B) schematic measurement for granulation tissue thickness and granulation gap[30, 31]. (C) Quantification of granulation tissue gap and thickness on day 7 and 20. **P < 0.01, *P < 0.05, n> 5.

In the final remodeling stage of wound healing, a mass deposition of collagen (a predominant structural protein in skin) is necessary to reconstruct dermal tissue at wound sites effectively. Masson's trichrome staining (MTS) on day 7 and day 20 were used to determine the histological collagen deposition (staining in blue). As shown in **Figure 6A**, on day 7, all polySBMA-treated wounds were covered by a more intense blue color as compared to the control group, demonstrating that collagen deposition was most enhanced in hydrogel-treated wounds, leading to the thicker wound granulation formation and the smaller wound gap. On day 20, the accelerated granulation tissue formation and collagen deposition became even more pronounced. Among four hydrogel-treated wounds, it can be seen that the softer hydrogel groups not only had the extensive and thick collagen deposition both in wound center and

wound edge reflected by the deep blue staining, but also the most orderly collagen arrangement compared with other groups at both 7 and 20 days. We also observed that the soft hydrogel-treated wounds had more densely packed collagen fibers with parallel arraignment as compared to the stiff hydrogel-treated wounds with loosely packed collagen fibers running in irregular arrangements, or control with nothing. Quantitatively, **Figure 6B** shows the statistical analysis of collagen deposition on day 20. Clearly, the mean collagen deposition density in PBS-, soft-1-, soft-2-, stiff-1-, and stiff-2-treated wounds was 4539.4 ± 1386.6, 42882.3 ± 15839.2, 15887.5 ± 6386.6, 11528.3 ± 1380.3, and 6091.7 ± 1526.0 /mm^2, respectively. So, the soft hydrogel-treated wounds represented 3-7 fold increase in collagen deposition, relative to the wounds treated with stiff hydrogels. These results confirm further the effectiveness of wound healing by wound remodeling via more collagen deposition. It is important to mention that, collective data from **Figure 4** (wound closure rate and image), **Figure 5** (granulation formation), **Figure 6** (collagen deposition) indicate that the wound in the control group on day 20 did not completely close, and the partial wound closure is likely due to the contraction effect the wound. We should also note that severed muscle and deeply stain with trypan does not necessarily indicate the existence of normal tissue, instead they could be an indicator of newly regenerated skins as well in our case.
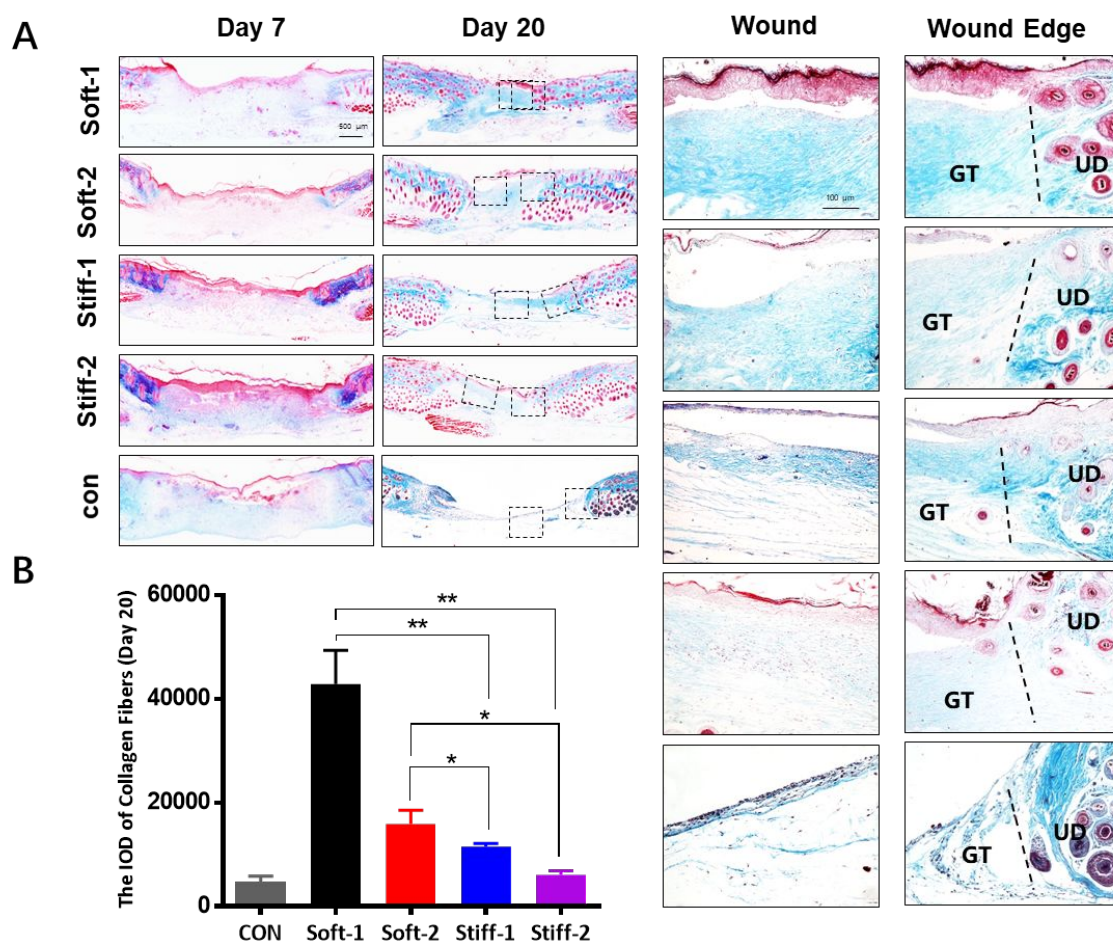
Figure 6. Masson's trichrome staining (MTS) of wound sections obtaining from different zwitterionic polySBMA hydrogels and control groups day 7 and day 20 post-operation, showing collagen deposition and maturity. (A) MTS images for skin wounds treated with polySBMA hydrogels and PBS on day 7 and day 20 (scale bar=500 μm), as well as a close-up MTS images at wound center and wound edge on day 20 (scale bar=100 μm). (B) Quantification of collagen deposit density in the wound sites on day 20 by optical blue density (IOD), **P < 0.01, *P < 0.05, n > 5.

3.4. Soft polySBMA hydrogels accelerat more neovascularization than stiff polySBMA hydrogels

Among the wound healing processes that could be triggered by GFs, neovascularization and angiogenesis are crucial to tissue engineering[32]. The formation of new vasculature is fundamental to powering the wound regeneration. To confirm the newly formed vessels found in wound area, we also performed immunofluorescence staining of CD31 endothelial cell marker to identify the new blood vessels formation on day 7. As shown in **Figure 7A**, wounds

treated with both softer hydrogels exhibited a higher amount of CD31 cells than wounds treated with stiffer hydrogels. To further assess this outcome, the overall area covered by the CD31 cells in the hydrogel groups was quantified to determine their density in the wound area. **Figure 7B** showed that the density of CD31 cells was 17.21%, 13.4%, 4.3%, and 1.7% for soft-1-, soft-2-, stiff-1-, and stiff-2-treated wounds, respectively, consistent with immunofluorescence staining images. Thus, the softer hydrogel wound dressings will promote angiogenesis and neovascularization, which in turn provide more oxygen and nutrients to the wounds and guide the cells for wound remolding such as granulation and collagen formation (**Figure 7C**). Thus, our results suggest that soft hydrogels accelerate wound healing *via* improved granulation tissue formation and epithelial tissue regeneration, possibly by increasing collagen deposition and the formation of new blood vessels.
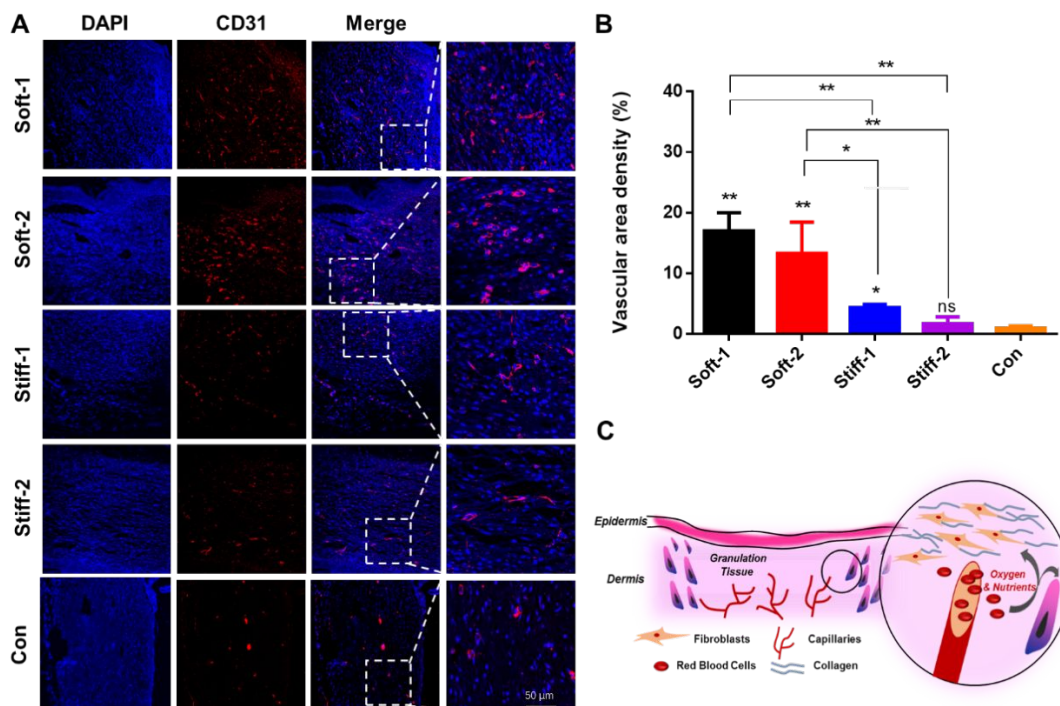
Figure 7. CD31 staining for characterizing neovascularization in wound sites of different zwitterionic polySBMA hydrogel and control group. (A) CD 31 (red) and DAPI (Blue) staining for new blood vessels on day 7 post-wound operation. (B) Quantitative analysis of newly formed blood vessels as measured by vascular area density on day 7. **P < 0.01, *P < 0.05, n>5. (C) Schematic of neovascularization at wound sites.

3.5. Soft polySBMA hydrogels enhance cell proliferation and M2/M1 macrophages than stiff polySBMA hydrogels

In order to further understand the mechanical regulation of wound healing mechanism. Ki-67 protein (also known as MKI67) was used as cellular maker for evaluating cell proliferation during the wound repair process. As shown in **Figure 8A**, soft-1 and soft-2 dressings up-regulated cell proliferation as compared to stiff-1 and stiff-2 dressings at early stage of wound healing on day 7, as evidenced by significant differences of *** $p < 0.001$ between soft-1 and two stiff hydrogels and of ** $p < 0.01$ between soft-2 and two stiff hydrogels, respectively (**Figure 8C**). In addition, these cells could further secret granulation matrix and different types of growth factors to promote wound regeneration. This enhanced cell proliferation once again confirms a beneficial role of soft polySBMA hydrogels in wound repair.

Macrophages activation of M2 (anti-inflammatory) versus M1 (pro-inflammatory) is considered as an important factor to promote angiogenesis and tissue remodeling. In our previous work, we have demonstrated that zwitterionic polySBMA hydrogel enable to pursue the polarization of macrophages from M1 to M2 through enhanced anti-inflammatory proteins to achieve wound pro-healing functions[33]. Here, we also quantified and compared M1 (stained by CD-68, red color) and M2 macrophage (stained by CD-163, green color) of the four hydrogels, as compared to the control group. It can be seen in **Figure 8 B&D** that the soft-1 and soft-2 dressings were much more active to up-regulate M2 macrophages at day 7 than the stiff-1 and stiff-2 dressings, as evidenced by the presence of more green color in **Figure 8B** and a significant difference of *** $p < 0.001$ between soft hydrogels and stiff hydrogels in **Figure 8D**. In line with wound closure rate, granulations formation, and collagen deposition, the results of the expression of M2/M1 macrophages again confirm the positive role of soft hydrogels in wound regeneration.

We also conducted cell toxicity experiments, when co-cultured with polySBMA hydrogels, to verify their biocompatibility. As shown in **Fig. S1-A**, as compared to the control group, four hydrogel groups showed no obvious differences in terms of the morphology and proliferation of Hacat cells. Furthermore, CCK-8 assay in **Fig. S1-B** showed that upon 24 h incubation, cell viability for all hydrogels groups and the control group displayed no obvious difference. Both cell toxicity and viability results indicate the good biocompatibility of

polySBMA hydrogels.
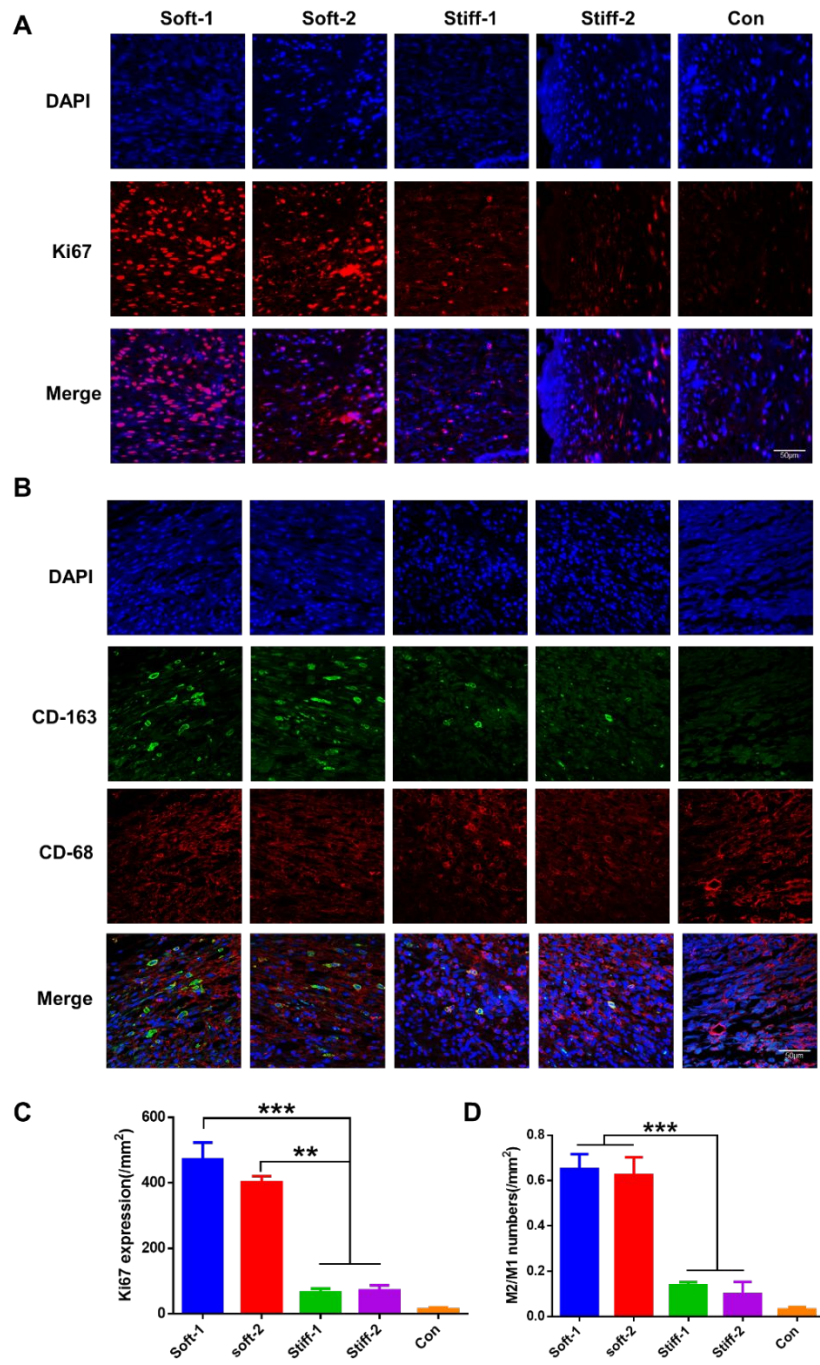
Figure 8. A) Immunofluorescent staining of wound sites on day 7 post-wounding for cell proliferation (Ki67, red) and stained nuclear with DAPI (blue). B) Immunofluorescent staining of wound sites on day 7 post-wounding for M1 (CD-68, red), M2 macrophage (CD-163, green) and stained nuclear with DAPI (blue). C) Quantitative evaluation of Ki67 expression of four hydrogels and the control on day 7. D) Quantitative evaluation of M2/M1 of four hydrogels and the control. Significant differences between samples are defined by *** $P < 0.001$, ** $P < 0.01$, where $n > 6$.

4. Conclusion

In this study, zwitterionic polySBMA hydrogels with different mechanical properties were prepared and used as wound dressings to treat the full-thickness dermal wound in mice. First, all polySBMA hydrogels demonstrated their high water content and retention ability, and super antifouling properties to prevent unwanted protein adsorption and cell adhesion *in vitro*. Then, the softer polySBMA hydrogels exhibited the better wound healing efficiency *in vivo* than the stiffer ones, through their enhanced wound closure, accelerated granulation tissue formation, increased collagen deposition, and improved new blood vessel formation. Finally, collective data revealed a correlation between mechanical property and wound healing efficiency, demonstrating a simple and possible generalizable approach to achieve the better wound healing efficiency by simply controlling mechanical property of hydrogels as wound dressings.

Reference

1. W. Loke, S. Lau, L. L. Yong, E. Khor and C. K. Sum, *Journal of Biomedical Materials Research*, 2000, **53**, 8-17.

2. P. S. Martin, *Science*, 1997, **276**, 75-81.

3. J. S. Boateng, K. H. Matthews, H. N. E. Stevens and G. M. Eccleston, *Journal of Pharmaceutical Sciences*, 2008, **97**, 2892-2923.

4. Y. H. Kim, K. T. Hwang, J. T. Kim and S. W. Kim, *Journal of Wound Care*, 2015, **24**, 536-542.

5. M. D. Konieczynska, J. C. Villacamacho, C. Ghobril, M. Perezviloria, K. M. Tevis, W. A. Blessing, A. Nazarian, E. K. Rodriguez and M. W. Grinstaff, *Angewandte Chemie*, 2016, **55**, 9984-9987.

6. N. Roy, N. Saha, T. Kitano and P. Saha, *Soft Materials*, 2010, **8**, 130-148.

7. B. Mirani, E. Pagan, B. Currie, M. A. Siddiqui, R. Hosseinzadeh, P. Mostafalu, Y. S. Zhang, A. Ghahary and M. Akbari, *Advanced Healthcare Materials*, 2017, **6**, 1700718.

8. S. Sakai, M. Tsumura, M. Inoue, Y. Koga, K. Fukano and M. Taya, *Journal of Materials Chemistry B*, 2013, **1**, 5067-5075.

9. T. S. Stashak, E. Farstvedt and A. Othic, *Clinical Techniques in Equine Practice*, 2004, **3**, 148-163.

10. S. A. Eming, P. Martin and M. Tomiccanic, *Science Translational Medicine*, 2014, **6**.

11. R. O. Hynes, *Science*, 2009, **326**, 1216-1219.

12. B. Cheng, M. Lin, G. Huang, Y. Li, B. Ji, G. M. Genin, V. Deshpande, T. J. Lu and F. Xu, *Physics of Life Reviews*, 2017, 88-119.

13. V. Llopishernandez, M. Cantini, C. Gonzalezgarcia, Z. A. Cheng, J. Yang, P. M. Tsimbouri, A. J. Garcia, M. J. Dalby and M. Salmeronsanchez, *Science Advances*, 2016, **2**.

14. J. Barthes, H. Ozcelik, M. Hindie, A. Ndreuhalili, A. Hasan and N. E. Vrana, *BioMed Research International*, 2014, **2014**, 921905-921905.

15. P. Olczyk, Ł. Mencner and K. Komosinskavassev, *BioMed Research International*, 2014, **2014**, 747584-747584.

16. G. Xia, Y. Liu, M. Tian, P. Gao, Z. Bao, X. Bai, X. Yu, X. Lang, S. Hu and X. Chen, *Journal of Materials Chemistry B*, 2017, **5**, 3172-3185.

17. S. Chen, J. Shi, X. Xu, J. Ding, W. Zhong, L. Zhang, M. Xing and L. Zhang, *Colloids and Surfaces B: Biointerfaces*, 2016, **140**, 574-582.

18. D. Y. Shu and F. J. Lovicu, *Progress in Retinal and Eye Research*, 2017, **60**, 44-65.

19. E. Hadjipanayi, V. Mudera and R. A. Brown, *Journal of Tissue Engineering and Regenerative Medicine*, 2009, **3**, 77-84.

20.   A. J. Engler, S. Sen, H. L. Sweeney and D. E. Discher, *Cell*, 2006, **126**, 677-689.

21.   R. G. Wells and D. E. Discher, *Science Signaling*, 2008, **1**.

22.   S. R. Peyton and A. J. Putnam, *Journal of Cellular Physiology*, 2005, **204**, 198-209.

23.   J. Wu, Z. Xiao, A. Chen, H. He, C. He, X. Shuai, X. Li, S. Chen, Y. Zhang and B. Ren, *Acta biomaterialia*, 2018, **71**, 293-305.

24.   H. He, X. Xuan, C. Zhang, Y. Song, S. Chen, X. Gong, B. Ren, J. Zheng and J. Wu, *Langmuir*, 2018, DOI: 10.1021/acs.langmuir.8b01755.

25.   J. Wu, J. Zhu, C. He, Z. Xiao, J. Ye, Y. Li, A. Chen, H. Zhang, X. Li and L. Lin, *ACS Applied Materials & Interfaces*, 2016, **8**, 18710-18721.

26.   J. Wu, J. Ye, J. Zhu, Z. Xiao, C. He, H. Shi, Y. Wang, C. Lin, H. Zhang, Y. Zhao, X. Fu, H. Chen, X. Li, L. Li, J. Zheng and J. Xiao, *Biomacromolecules*, 2016, **17**, 2168-2177.

27.   J. Wu, C. Zhao, W. Lin, R. Hu, Q. Wang, H. Chen, L. Li, S. Chen and J. Zheng, *Journal of Materials Chemistry B*, 2014, **2**, 2983-2992.

28.   J. Wu, C. Zhao, R. Hu, W. Lin, Q. Wang, J. Zhao, S. M. Bilinovich, T. C. Leeper, L. Li and H. M. Cheung, *Acta biomaterialia*, 2014, **10**, 751-760.

29.   L. Li, S. Chen, J. Zheng, B. D. Ratner and S. Jiang, *Journal of Physical Chemistry B*, 2005, **109**, 2934-2941.

30.   X. Zhao, H. Wu, B. Guo, R. Dong, Y. Qiu and P. X. Ma, *Biomaterials*, 2017, **122**, 34-47.

31.   J. Devalliere, K. Dooley, Y. Hu, S. S. Kelangi, B. E. Uygun and M. L. Yarmush, *Biomaterials*, 2017, **141**, 149-160.

32.   J. Li, Y. P. Zhang and R. S. Kirsner, *Microscopy research and technique*, 2003, **60**, 107-114.

33.   J. Wu, Z. Xiao, A. Chen, H. He, C. He, X. Shuai, X. Li, S. Chen, Y. Zhang and B. Ren, *Acta Biomaterialia*, 2018, **71**, 293-305.

TOC